# Acoustic Source Localization System Using A Linear Arrangement of Receivers for Small Unmanned Underwater Vehicles

Bobby Hodgkinson[1,3], David Shyu[2,3], and Kamran Mohseni[1,2,3]

[1]Department of Mechanical and Aerospace Engineering
[2]Department of Electrical and Computer Engineering
[3]Institute for Networked Autonomous Systems
University of Florida
Gainesville, FL 32611

***Abstract*—An acoustic localization system using a linear hydrophone array is presented which has been designed to provide three dimensional positioning information relative to a signal source for testing in confined environments such as swimming pools or water tanks. The system is designed to fit within the size, power, and computational limitations of resource constrained small underwater vehicles. The feasibility of the technique was demonstrated in a confined test environment with severe multipath signals. Experimental test results in a 8 m diameter, 4.5 m deep steel tank show localization errors of less than 5% of the slant range which is comparable to commercially available systems designed for large vehicles in the open ocean.**

## I. Introduction

A great deal of successful work has been done over the last several decades in underwater acoustic communication systems and localization systems. Milne [1] categorizes underwater positioning system into three main classes. The long baseline (LBL) systems uses multiple transmitters or receivers spaced several meters apart. Simple geometry and the round trip travel time of an acoustic signal can be used to locate a submersible relative to the baseline array. Ultra-short baseline (USBL) systems use a tightly packed array of receivers to determine the angle at which a signal arrives based on the phase difference of the signal at each of the receivers. Combined with the round trip travel time of the signal the location of the submersible can be determined accurately. Short baseline systems (SBL) use an array of multiple receivers and geometry similar to the LBL technique to unique position a submersible.

In many applications the receiver array of these systems is typically housed on a large mothership [2], [3]. A simple transponder is placed on the submersible to allow the mothership to position the submersible with respect to the mothership. Variations of these techniques have also been widely demonstrated where the submersible positions itself relative to the mothership. The convention is to simply place the word 'inverted' in front of the categorization such as 'inverted Ultra-short baseline' or iUSBL [4].

Several companies exist that manufacture and sell high-quality, reliable underwater wireless positioning systems for underwater vehicles [5]. Unfortunately for small (1 meter in length) autonomous underwater vehicle designers, the majority of commercially available systems focus on applications regarding relatively large vehicles in the open ocean. Adaptation of commercially available systems would require significant modification in order to fit within the size, power, and processing limitations of small underwater vehicles.

For the purposes of small autonomous underwater vehicles (AUVs) it is more desirable for the vehicles to position themselves relative to a known location than to have a mothership relay the vehicle's position relative to the mothership [6]. Furthermore, for underwater vehicle testing in confined environments multipath and the acoustic reverberation time are major concerns. In these confined environments the time required for an acoustic signal to decay below the noise threshold can be on the order of several tens of milliseconds [7], [8]. With these concerns in mind there exists a niche for a small, passive localization device that is able to fit within the limitations of resource constrained vehicles tested in confined environments such as swimming pools and small tanks. To the author's knowledge there does not exist a commercially available localization system capable of satisfying the strict size requirements of small AUVs such as the Cephalobot vehicle [9]. Moreover, the amount of multipath present in confined testing environments such as swimming pools and water tanks warrants a robust processing scheme.

This article builds upon work by the authors regarding a low cost in-house developed (iUSBL) system for small unmanned submersibles. The previous arrangement was comprised of a triangular array of hydrophones and an acoustic projector on the underside of the vehicle similar to systems employed on large scale ships [7], [9]. The primary improvement to the system is a more advanced signal processing scheme which provides increased localization accuracy and precision.

The remainder of this paper is organized as follows: section II provides an outline of the primary motivation for this work, section III derives the localization technique using geometry and time difference of arrival, section IV details the signal

978-1-4673-0831-1/12/$31.00 ©2012 IEEE

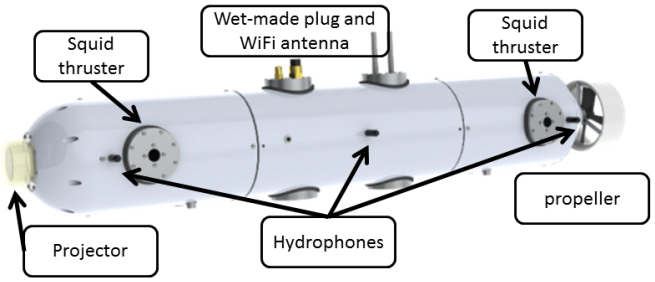


Fig. 1: The Cephalobot vehicle is a 1 meter long, 0.15 meter diameter autonomous underwater vehicle equipped with squid inspired vortex ring thrusters [9]. The vehicle is equipped with a National Instruments sbRIO 9632 main processor, wireless antenna for surface communication, forward and downward looking cameras, and a VectorNAV VN-100 IMU/digital compass.

processing scheme used to verify the feasibility of the localization technique using experimental data and analyzes the results of field experiments. Finally section V provides several options to improve the technique and supporting simulations and experiments of these improvements.

## II. Motivation

The primary motivation for this work is to provide a localization system for small unmanned underwater vehicles used as experimental testbeds in confined pools or water tanks. The vehicles will be tested in a shallow (4.5 meter deep) environment making multipath a significant concern.

The strict bandwidth limitations of the underwater environment make it less desirable to transmit positioning information when that same information can be obtained using the signal itself [6]. In the proposed system localization and communication can be conducted using the same acoustic signal. The first portion of the signal is used to determine the time difference of arrival at receivers and the later portion of the signal can be used to encode data. The focus of this article is on the localization scheme and the communication scheme will be a focus of future work.

In the author's previous work an array of hydrophones spaced 3 cm apart in an iUSBL arrangement and a projector were placed on the underside of the vehicle. It was experimentally determined that an increased spacing of the hydrophones would yield increased positional accuracy. The increased hydrophone spacing would require a decrease of signal frequency to maintain the $\frac{1}{2}$ wavelength requirement of iUSBL systems. Unfortunately, it was experimentally observed that a lower signal frequency increases the effects of multipath rendering a low frequency iUSBL system impractical for a confined test environment. These considerations lead to the arrangement of small hydrophones placed in a linear fashion and a signal projector placed in the nose as shown in Figure 1 on the 1 meter long Cephalobot vehicle. Figure 1 shows the port side hydrophones and the starboard side would be mirrored.

## III. Methodology

### A. Algorithm derivation

Figure 2 provides a schematic of the variables used in the derivation of the linear array localization algorithm. The algorithm is developed for $i$ total sensors but it will be shown that 3 sensors is sufficient to accomplish the positioning goals of the system. Obviously a larger number of sensors would introduce redundancy and potentially reduce the localization error. The sensors are defined as $1, 2, \cdots, i$ and the signal source defined as element 0. The inter-element spacing $d_{i(i+1)}$ is constrained to the $x$-axis which is defined along the length of the elements. Assuming a constant speed of propagation ($u_s$) let $d_{0i}$ denote the distance between the source and the $i$th element and $t_i = \frac{d_{0i}}{u_s}$ is the time when the signal reaches the $i$th element. The time difference $\tau_i$ of the received signal at consecutive receivers is simply the difference between $t_i$ and $t_{i+1}$. Using geometry it can be shown that the location of the source in the $x$-direction $x_0$ and the distance $d_{01}$ can be written as:

$$x_0 = \frac{A(e-b)}{c(e-b)-(bf)}, \tag{1}$$

$$d_{01} = \frac{fx_0 + g - e^2 + b^2}{2e - 2b}, \tag{2}$$

where

$$\begin{aligned} b &= u_s\tau_1, \\ c &= -2d_{12}, \\ d &= d_{12}^2, \\ e &= u_s(\tau_1+\tau_2), \\ f &= -2d_{23}, \\ g &= d_{23}(d_{23}+2d_{12}), \\ A &= \frac{bg - be^2 - b^3}{e-b} + b^2 - d. \end{aligned}$$

With knowledge of the difference in vehicle depth and signal source depth ($z_0$) the $y$-component of the source location can be found as equation 3. This equation has two solutions but only one solution is realized in practical applications since the receivers are assumed to receive signals only in the $+y$-direction due to the location on the vehicle.

$$y_0^2 = d_{01}^2 - x_0^2 - z_0^2 \tag{3}$$

### B. Signal Processing

The time delay of arrival of the signal from the projector at each of the receivers and the difference in depth between the projector and receiver array are the only unknowns required to uniquely determine the location of the signal source. For experimental demonstration the depth of the projector remained at a constant 1 m below the receiver array. In future deployments the depth of the signal source will be encoded in the signal immediately after the localization portion of the signal. The depth of the array will be known from the

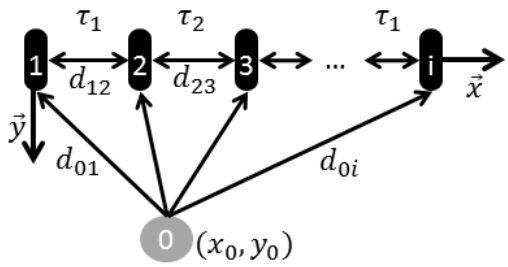


Fig. 2: Linear array definition. $\vec{x}$ direction along length of array, $\vec{y}$ perpendicular to $\vec{x}$ in the horizontal plane, $\vec{z}$ completes right hand rule.

Fig. 3: 8 m diameter, 4.5 m deep underwater vehicle testing tank located at the University of Florida.

vehicle's depth sensor thus transforming 3D localization to its 2D counterpart similar to [10].

Several options are available to filter and determine the time difference of multiple signals. Here, we employ an easy approach by using an inverse FFT lowpass filter to eliminate frequencies greater than 35kHz and cross correlation to determine the time offset of the signals which is similar to the approach in [11]. Since the time offset of the signals is determined by finding the lag corresponding to the maximum peak in the cross correlation spectrum it is desirable to use a signal that has a single peak in the cross correlation spectrum. Using a similar processing technique [12] showed promising experimental results using several different types of signals including: pseudo-random binary sequence, linear chip, logarithmic chip, etc. We have chosen to implement a linear chirp due to the desirable properties in the cross correlation spectrum. In order for the technique to function well the assumption that the signal level is greater than any multipath signal within the cross correlation data set must be made.

## IV. Experiment Results

The technique was tested in a 8 meter diameter, 4.5 meter deep steel tank shown in Figure 3. Three Reson 4013 hydrophones were placed 0.5 meter apart and held stationary throughout the test at a depth of 0.3 m. An in house developed projector was constructed by potting a cylindrical piezoceramic in Clear-Flex 95 epoxy using a similar method as in [13]. The projector was placed at different locations in the testing tank at a depth of 1.3 m. The signal supplied to the projector was a set of two linear chirps played back to back sweeping between 25kHz and 18kHz each lasting 500 $\mu s$ for a total signal duration of 1 ms. The signal was amplified to approximately $\pm$90 V by a $\times$10 voltage amplifier in order to obtain a noticeable signal at the hydrophone output.

The signal was repeated at 1 Hz to allow multipath signals to decrease well beneath the noise floor. The received signals were captured and stored using an oscilloscope with a sample rate of 1MS/s per channel. The supply signal to the projector was used to trigger the data capture of the scope as a way to synchronize the data between experiments. This triggering scheme was employed in order to simplify the post processing and to eliminate the potential of capturing multipath signals instead of the projector signal.

The signals for a typical test are shown in Figure 4. The upper three plots show the output voltage from the three hydrophones. The lower plot shows the signal supplied to the projector to provide a reference as to the signal start time. For this particular test, the separation between the projector and the receiver array was measured to be 4.5 m. The signal arrives at the hydrophones approximately 3 ms after it is sent from the projector which is consistent with the acoustic speed of propagation in water. The most notable feature of the signals shown in Figure 4 is the multipath signals present approximately 2 ms after the initial signal arrival. The precise source of this multipath is difficult to identify but the most likely source is from the tank wall. For this particular experiment, the separation between the projector and the tank wall was approximately 1.5 m which would add an additional 2 ms of signal travel time consistent with the multipath observation.

Due to the high amount of multi-path experienced in the experiments the cross correlation of the entire filtered signal often yields incorrect results. The lag time associated with the maximum amplitude of the cross correlation corresponds to the time difference between the two signals. Figure 5 shows the cross correlation spectrum of the filtered data shown in Figure 4. The solid line is the cross correlation of the upper two plots in Figure 4 (hydrophone signals 1 and 2) and the dashed line is the cross correlation of the middle two plots (hydrophone signals 2 and 3). The cross correlation of hydrophone signals 2 and 3 does not yield a well defined dominant peak but the cross correlation of hydrophone signals 1 and 2 does. For this particular test the cross correlation method yields a time difference of 0.3 ms between signals 1 and 2 and -0.25 ms between signals 2 and 3 which corresponds to an incorrect

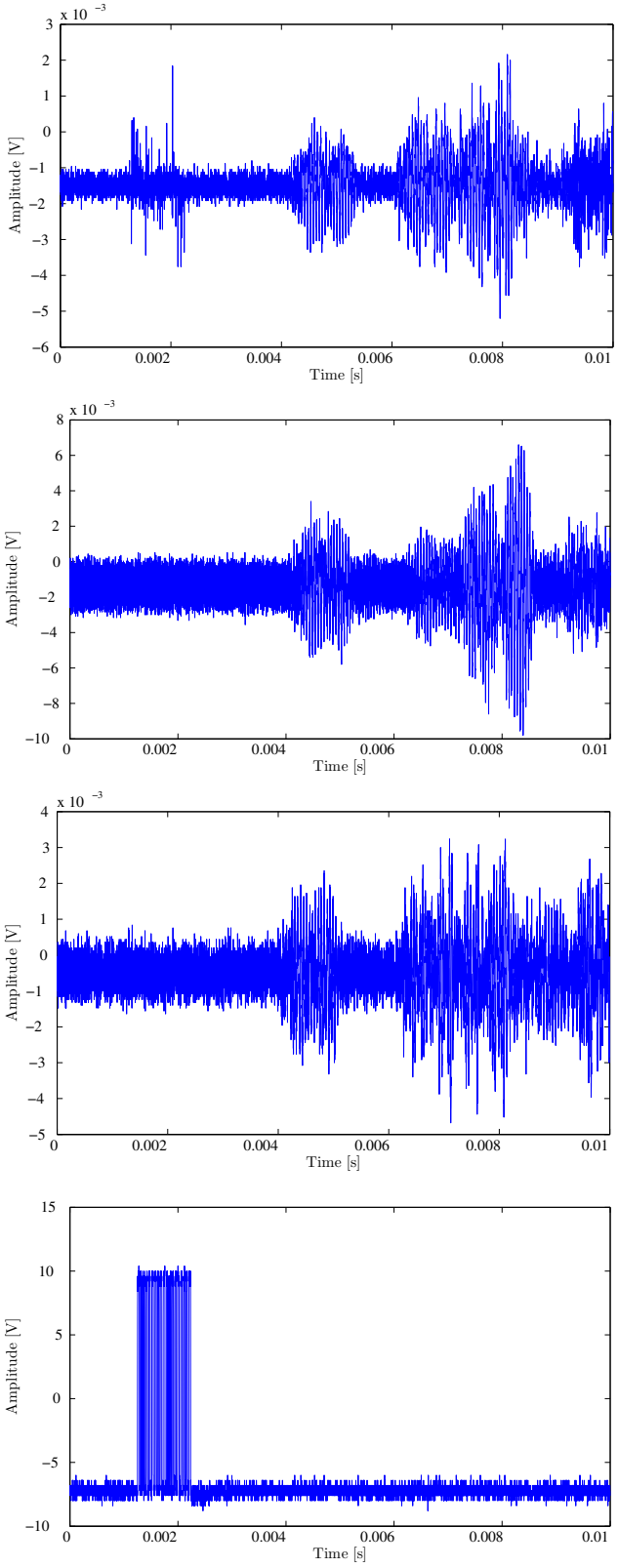


Fig. 4: Voltage levels versus time for three hydrophones (top three figures) and for the signal supplied to the projector (bottom figure) during a typical experiment. The supply signal was a set of two linear chirps from 25 kHz to 18 kHz each lasting 500 $\mu$s for a total signal duration of 1 ms. The signal arrives at each of the three hydrophones after approximately 3 ms. Multipath signals arrive at the receivers approximately 2 ms after the signal from the projector. The source of the multipath signal is most likely from the steel wall of the tank. The distance between the projector and the wall was approximately 1.5 meter which would add approximately 2 ms of signal propagation time to the signal. Furthermore the multipath signal is at times greater than the projector signal making signal processing difficult.

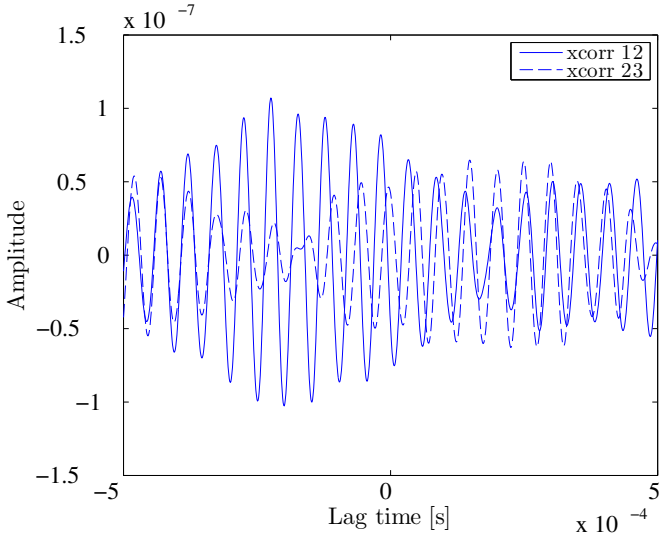


Fig. 5: The cross correlation spectrum of hydrophone signals 1 and 2 (solid line) and signals 2 and 3 (dashed line) for the signals shown in Figure 4. The signals were filtered using an inverse FFT filter set at 35 kHz. The lag time associated with the maximum amplitude represents the estimated time difference of arrival between the respective hydrophones using the entire signal (multipath included). This results in a time difference of 0.3 ms between signals 1 and 2 and -0.25 ms between signals 2 and 3 which is incorrect due to the multipath signal.

location of approximately $(0.46, 0.28)$m.

In order to eliminate the multi-path signals the experimental data was passed through a window function which eliminated all the data after a specified sample number. Figure 6 shows the cross correlation for the aforementioned signals after eliminating all data after a time of 0.006 s. For both cross correlations there now exists a clear maximum. The lag time corresponding to these maximums correspond to a time difference of 0.05 ms and 0.085 ms for signals 1 and 2 and signals 2 and 3 respectively. These time differences correspond to an estimated signal location of $(1.75, 4.75)$ m.

Figure 7 shows the results of the calculated position (blue markers) in the horizontal plane with the independently measured position of the projector (red marker) and the outline of the testing tank (blue circular outline). The projector was placed at 6 different locations in the testing tank. The first location $(2.5, 2)$ m is indicated by a large red $\diamond$. The smaller blue $\diamond$s indicated the calculated projector location based on the time difference of arrival for 5 separate data sets with the projector at $(2.5, 2)$m. The projector was then moved to $(2.5, 2.75)$m (indicated as a large red $\triangle$) and 5 samples were gathered. Smaller blue $\triangle$ indicate the calculated location of the signal source with the projector at $(2.5, 2.75)$m. The experiment was then repeated at the locations indicated by the $\triangleright$, $\circ$, $+$, and $\times$ in that order. Black $\bullet$ represent the individual hydrophone locations with hydrophone 1 at $(0, 0)$.

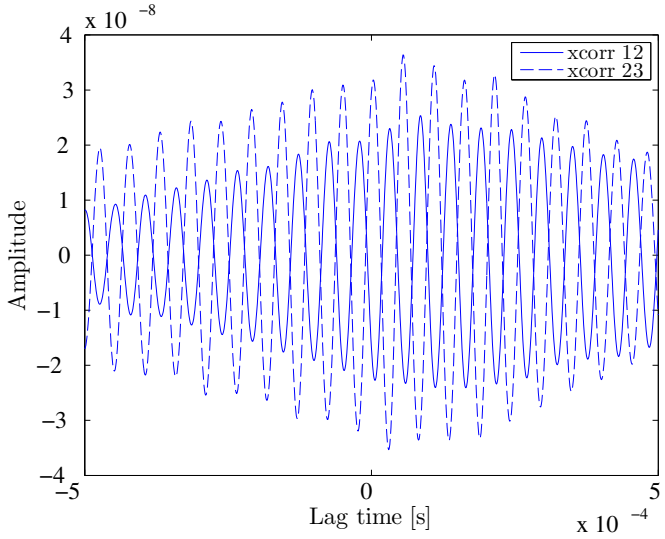


Fig. 6: The cross correlation spectrum of hydrophone signals 1 and 2 (solid line) and signals 2 and 3 (dashed line) for the signals shown in Figure 4. The signals were filtered using an inverse FFT filter set at 35 kHz and a window function to eliminate all signals after 6 ms. The lag time associated with the maximum amplitude represents the estimated time difference of arrival between the respective hydrophones using this signal (multipath excluded). This results in a time difference of 0.05 ms between signals 1 and 2 and 0.085 ms between signals 2 and 3. The time of arrival estimate yields a positioning estimate of the projector in reference to the hydrophone array within 2.5 cm in the $x$-direction and 12.5 cm in the $y$-direction of the measured location.

Close groupings of similar blue markers with the larger red markers indicate high precision and accuracy of the technique. Figure 8 shows the calculated time differences ($\tau_1$ and $\tau_2$) of the signals received for different projector locations. Close groupings of signals indicate a high level of repeatability in the technique. The markers correspond to the locations shown in Figure 7.

Figure 7 shows consistency between data sets but does provide a quantifiable comparison between similar systems. A common standard of underwater positioning systems is to report the accuracy in reference to the slant range between the source and receiver. The independently measured location of the projector is used to calculate the reference slant range $R$ as

$$R = \sqrt{x^2_{\text{projector}} + y^2_{\text{projector}} + z^2_{\text{projector}}} \tag{4}$$

Let $x_{\text{error}}$ denote the error in the $x$-direction defined as the difference between the calculated $x$-location and the measured $x_{\text{projector}}$ (likewise for $y_{\text{error}}$). This yields an $x$ and $y$ accuracy in reference to slant range as

$$x_{\text{accuracy}} = \frac{x_{\text{error}}}{R} * 100\%, \tag{5}$$

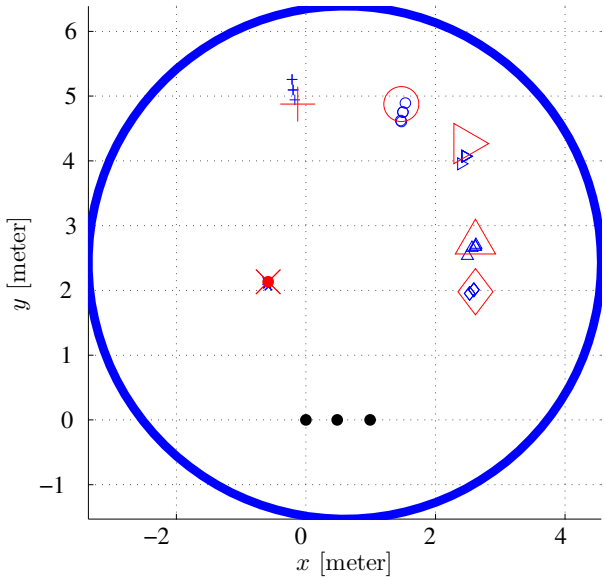


Fig. 7: The calculated locations of the source based on the signal time difference or arrival. The projector was placed at 6 different locations in the testing tank. The first location $(2.5, 2)$ m is indicated by a large red $\diamond$. The smaller blue $\diamond$s indicated the calculated projector location based on the time difference of arrival for 5 separate data sets with the projector at $(2.5, 2)$m. The projector was then moved to $(2.5, 2.75)$m (indicated as a large red $\triangle$) and 5 samples were gathered. Smaller blue $\triangle$ indicate the calculated location of the signal source with the projector at $(2.5, 2.75)$m. The experiment was then repeated at the locations indicated by the $\triangleright$, $\circ$, $+$, and $\times$ in that order. Black $\bullet$ represent the individual hydrophone locations with hydrophone 1 at $(0, 0)$. Close groupings of similar blue markers with the larger red markers indicate high precision and accuracy of the technique. The sample voltages shown in Figure 4 corresponds to an experiment shown here as a $\circ$.

and

$$y_{\text{accuracy}} = \frac{y_{\text{error}}}{R} * 100\%. \tag{6}$$

The results shown in Figure 7 exhibit an $x_{\text{accuracy}}$ of $\pm$ 2% and a $y_{\text{accuracy}}$ of $\pm$5% which is of the same order of accuracy of commercially available systems [14]. The results experimentally validate the methodology derived in section III and also demonstrate the use of iFFT and cross correlation to determine a time difference of arrival of underwater acoustic signals in an environment with severe multipath. Nevertheless the signal processing scheme requires improvement prior to implementation on an underwater vehicle. In the following we present one possible approach and supporting experimental results.

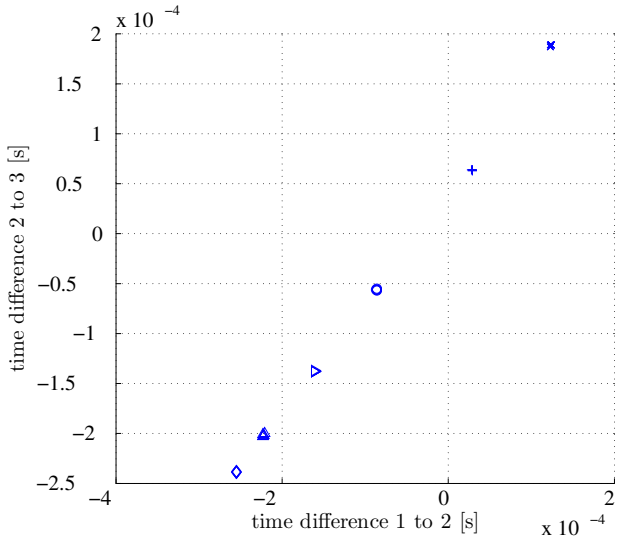


Fig. 8: The calculated time difference of signals for different projector locations. At each projector location 5 data sets were gathered and close groupings of markers indicate high repeatability in the processing scheme. The sample voltages shown in Figure 4 corresponds to an experiment shown here as a ○. Markers correspond to the test locations shown in Figure 7.

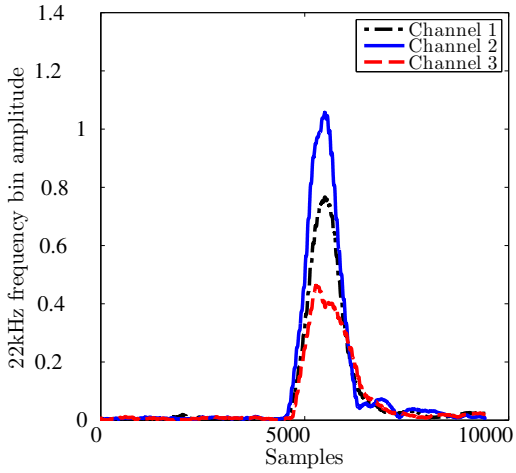


Fig. 9: SDFT sample result for a typical test case with the source approximately in line with hydrophone 2 at a separation of approximately 2 meters. Hydrophone signal 1 is shown as the black dash/dot line, signal 2 as the blue solid line and signal 3 as the red dashed line. The multiple local maximums in the SDFT are an undesirable result of extra cycles present in the signal. Due to this phenomenon a threshold crossing scheme was employed which found the time associated when the SDFT magnitude crosses 0.05 to calculate the time delay of the signal arrival.

## V. Signal Processing Improvements

The aforementioned processing scheme is able to yield localization results which are comparable to commercially available systems. However, the technique is not yet feasible for deployment on an autonomous underwater vehicle primarily due to the inability of the scheme to eliminate multipath effects prior to cross correlation. Recently a Sliding Discrete Fourier Transform (SDFT) was demonstrated to determine the time difference between acoustic signals in real time [15]. The SDFT is a common way of analyzing short instances of a signal in the frequency domain. In our application as in [15] we keep track of the magnitude of a specific frequency bin throughout the signal duration. In [15] the duration of the signal was used as the number of samples for the SDFT. This method produces a well defined peak in the frequency versus time relationship assuming the signal is not longer than expected. The times associated with these peaks for two different signals can then be used to determine the time difference of arrival.

In this experiment, the same hydrophone array was used; however, the source was not a linear chirp. Instead a regular sine wave of 5 cycles at 22kHz was used in order to yield a more ideal signal for the DFT. Ideally, the SDFT uses the location of the maximum amplitude of the desired frequency to calculate delays. However, in the experimental setup, the location of the maximum was affected by the projector resonant frequency and other environmental effects. Specifically it was noted that the received signal was anywhere between 7 cycles and 14 cycles and was not consistent between data sets. This phenomenon yielded multiple peaks after taking the SDFT and the maximum peak often yielded incorrect time differences.

Figure 9 shows the SDFT results for a sample test case where the source was approximately in line with the center hydrophone (channel 2). Channel 2 is expected to have the earliest maximum and channels 1 and 3 would have roughly equivalent maximum locations. However, depending on the amplitudes of the extra cycles, the calculated maximum could be delayed from the expected maximum. Further observation revealed that the SDFT of the channel that should arrive first began increasing first regardless of extra cycles in the signal and even multipath. Using a simple threshold value and identifying the sample where each channel crossed the threshold value, relatively consistent time differences were extracted. Figure 10 shows the measured location of the source and the estimated locations from the time difference of arrival using the SDFT threshold crossing method.

The resulting $x_{accuracy}$ and $y_{accuracy}$ using the SDFT threshold method were calculated to be 1.5% and 5% respectively. Despite the fact that an offset was observed between the calculated locations and the measured projector locations, the positioning results using SDFT are as precise as the cross correlation method. Nevertheless, the SDFT method is well suited for real time signal processing and is computationally inexpensive enough to run in real time aboard a resource constrained small underwater vehicle.

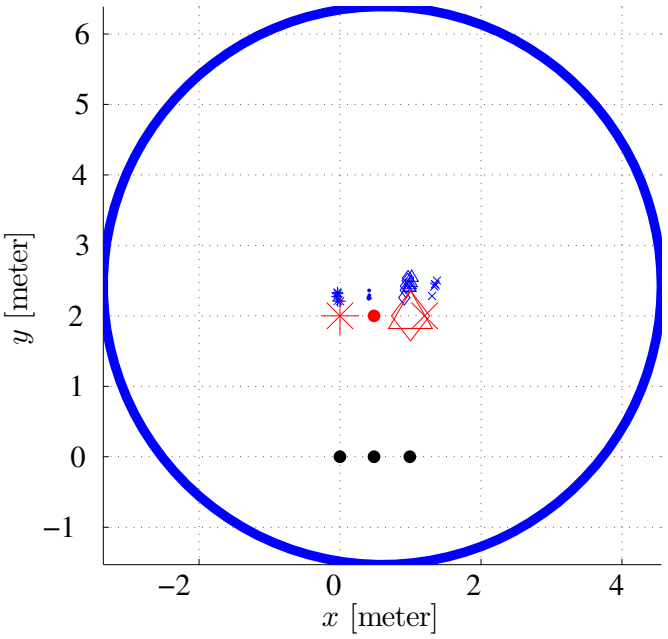


Fig. 10: Locations of the signal source based on time difference of arrival calculations using the SDFT signal processing method. The projector was placed at 5 different location in the testing tank. The first location $(0, 2)$m is indicated by a large red $*$. Smaller blue $*$ indicate the calculated projector location based on the time difference of arrival for 5 separate data sets with the projector at $(0, 2)$m. The projector was then moved to the locations indicated by the $\bullet$, $\diamond$, $\triangle$, and the $\times$ in that order. 5 data sets were recorded at each projector location. The close groupings of respective blue markers are of the precision as Figure 7 indicating similar positioning performance as to the cross correlation method.

## VI. Conclusion

This paper presents an underwater acoustic localization technique that is well suited for resource constrained vehicles in confined testing environments such as swimming pools and water tanks. The initial signal processing scheme yielded position errors on the order of 5% of the slant range between source and receiver array. This error is comparable to commercially available systems but the initial processing scheme required manual elimination of multipath effects on the signal.

A Sliding Discrete Fourier Transform (SDFT) was experimentally determined to provide similar positioning precision. The SDFT adds the potential for real time signal processing and a combined approach of cross correlation and SDFT will be a focus of future work. Additional future work will include designing hydrophone signal amplification and conditioning circuitry as well as embedded processing software. These advancements will allow for the implementation of the technique on an autonomous underwater vehicle.

## VII. Acknowledgments

The authors would like to acknowledge the Office of Naval Research (ONR) for funding support of this project.

## References

[1] P. Milne, "Underwater acoustic positioning systems," 1983.
[2] M. Audric, "Gaps, a new concept for usbl [global acoustic positioning system for ultra short base line positioning]," in *OCEANS'04. MTTS/IEEE TECHNO-OCEAN'04*, vol. 2. IEEE, 2004, pp. 786–788.
[3] K. Vickery, "Acoustic positioning systems. a practical overview of current systems," in *Autonomous Underwater Vehicles, 1998. AUV'98. Proceedings Of The 1998 Workshop on*. IEEE, 1998, pp. 5–17.
[4] T. Bennetts, "Applications of iusbl technology overview."
[5] C. Bussman, R. Burns, C. Knight, M. Ventura, C. Covey, R. Conward, J. Ortega, A. Barsotti, and S. Ingle Owen, "Sea technology buyers guide directory 2012."
[6] H. Tan, R. Diamant, W. Seah, and M. Waldmeyer, "A survey of techniques and challenges in underwater localization," *Ocean Engineering*, vol. 38, no. 14, pp. 1663–1676, 2011.
[7] D. Ambrosio, R. D. Gizzi, B. Hodgkinson, J. Kirkpatrick, C. Miller, J. Price, and T. Thomas, "Cuboat: Colorado underwater buoyant oceanic acoustic network," in *49th Aerospace Science Meeting Including the New Horizons and Aerospace Exposition*, January 2011.
[8] G. Curtis, "Reverberation characteristics of 4 khz and 20 khz tone bursts in a water filled tank and their effect on experimental design," *Acoustics, Speech and Signal Processing, IEEE Transactions on*, vol. 28, no. 3, pp. 324–327, 1980.
[9] M. Krieg, P. Klein, R. Hodgkinson, and K. Mohseni, "A hybrid class underwater vehicle: Bioinspired propulsion, embedded system, and acoustic communication and localization system," *Marine Technology Society*, pp. 153–164.
[10] W. Cheng, A. Teymorian, L. Ma, X. Cheng, X. Lu, and Z. Lu, "Underwater localization in sparse 3d acoustic sensor networks," in *INFOCOM 2008. The 27th Conference on Computer Communications. IEEE.* Ieee, 2008, pp. 236–240.
[11] M. Morgado, P. Oliveira, and C. Silvestre, "Experimental evaluation of a usbl underwater positioning system," in *ELMAR, 2010 PROCEEDINGS*. IEEE, 2010, pp. 485–488.
[12] N. Kottege and U. Zimmer, "Underwater acoustic localization for small submersibles," *Journal of Field Robotics*, vol. 28, no. 1, pp. 40–69, 2011.
[13] B. Benson, "Design of a low-cost underwater acoustic modem for short-range sensor networks," Ph.D. dissertation, University of California, San Diego, 2010.
[14] "Evologics usbl-series underwater acoustic device product information."
[15] S. Assous and L. Linnett, "High resolution time delay estimation using sliding discrete fourier transform," *Digital Signal Processing*, 2012.